

# New methodology for AC-pulsed GMAW parameterization applied to aluminum shipbuilding

Jair Carlos Dutra<sup>1</sup> · Régis Henrique Gonçalves e Silva<sup>1</sup> · Bruna Martinello Savi<sup>1</sup> · Cleber Marques<sup>1</sup> · Orestes Estevam Alarcon<sup>1</sup>

Received: 3 December 2014 / Accepted: 26 March 2015  
© The Brazilian Society of Mechanical Sciences and Engineering 2015

**Abstract** AC-pulsed gas metal arc welding may be a good option for applications that require low heat input and high productivity. The introduction of a negative polarity period assists in obtaining such characteristics, due to an increase in the wire melting rate for this polarity. The main difficulty related to the use of this version of the process is in selecting the correct welding parameters. In the scope of a medium scale (60 ft) R&D aluminum sailboat construction project, this paper deals with this issue—a tested calculation methodology for the 5087 naval aluminum alloy welding wire-electrode is proposed. By knowing the wire melting rate in both polarities, as well as the definition of some input parameters [pulse parameters, drop diameter, and negative electrode percentage (%EN)], it was possible to achieve other process variables (base current, base current time, negative current, and negative current time). The method was evaluated for different current waveforms and different negative electrode percentages. The results were satisfactory with good arc stability and the possibility of controlling the heat input in the workpiece.

**Keywords** Naval aluminum alloys · Shipbuilding · AC-pulsed GMAW · Synergistic program · 5087 Welding wire

---

Technical Editor: Alexandre Mendes Abrao.

---

✉ Bruna Martinello Savi  
brunamsavi@hotmail.com

<sup>1</sup> LABSOLDA—Welding and Mechatronics Institute, Mechanical Engineering Department, UFSC, Florianópolis, Santa Catarina, Brazil

## 1 Introduction

The constant need for higher levels of production and product quality in the naval sector, as well as the emerging of new materials drives the market to develop several versions of the traditional welding processes aiming to meet these requirements. In terms of the gas metal arc welding (GMAW) process, these innovative versions are basically related to the metal transfer mode and to the development of waveforms that improve the process control and overall performance. This ability to work more accurately with the welding parameters is mainly due to the evolution of control and power electronics, software and computerized systems that, when applied to the arc welding sector, allow the manufacture of modern, versatile welding power sources.

With regard to arc welding of aluminum alloys, problems related to their physical properties are common, particularly in relation to their thermal conductivity. In the case of thin sheets, this characteristic can cause burnthrough and lead to distortion risk. For this reason, penetration and heat input control are distinctions in these applications. Within this context, authors like Kumar et al. [1] who evaluated this process for thin aluminum alloy sheets, and Tong et al. [2] who observed higher productivity due to a high wire melting coefficient, refer to the use of the AC-pulsed GMAW process as a promising solution to the drawbacks. Besides the weld penetration and heat input control to the workpiece, the method results in productivity increases, since there is an increase in the melting rate via the use of alternating current (negative and positive polarity).

One sector where aluminum finds increasing application is shipbuilding, due to its aforementioned physical properties of high corrosion resistance and high mechanical properties to density ratio. In this context, the present work was carried out as a part of the construction project of a medium

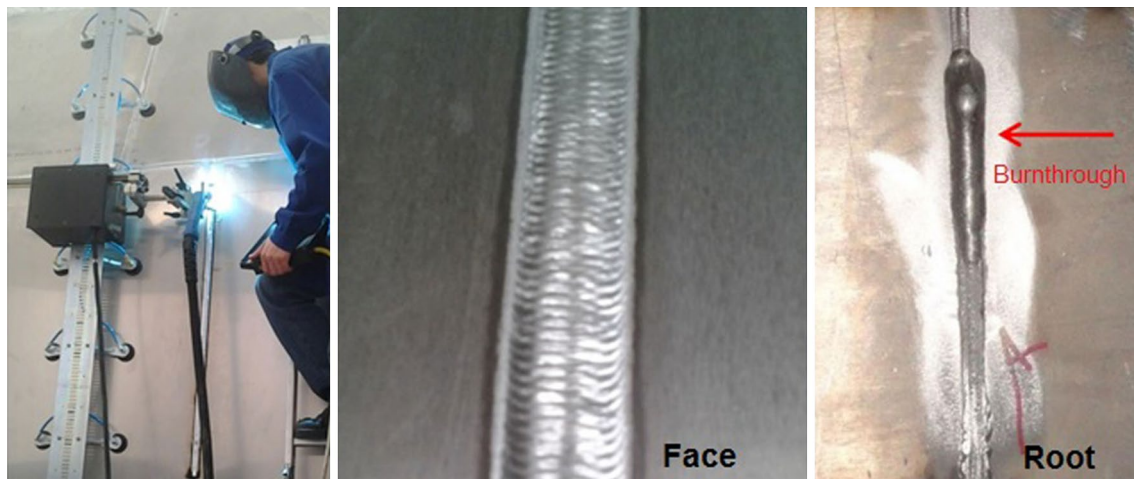


**Fig. 1** Automated DC-pulsed GMA welding process on the hull of the aluminum sailboat and details of burnthrough

scale (60 ft) R&D aluminum sailboat, which will serve as a mobile platform for sea exploration and alternative energies research for the Federal University of Santa Catarina, Brazil. The construction phase itself consisted in a R&D Project, aimed at developing welding automation devices and techniques, as well as welding processes. One of the technological needs that emerged concerned the filling passes for the V butt joints on the hull. Even in the presence of the root pass (performed with the CMT process), burnthrough arose as a potential problem when DC-pulsed GMAW was applied, as can be seen in Fig. 1, on a weld carried out on the sailboat's hull (8.0 mm sheet thickness).

The introduction of the AC-pulsed GMAW was then considered as a solution for the accomplishment of the hull welds for its properties of low heat input and high productivity.

Basically with regard to metal transfer, AC-pulsed GMAW utilizes the fundamental assumptions employed by DC-pulsed GMAW; that is, one drop per pulse (ODPP) detachment and equality between wire feed rate and wire melting rate [3]. The main difference of the AC in relation to the DC mode is the introduction of a negative polarity time in the current range (negatively polarized wire-electrode). With this inversion, the advantages of using each polarity are combined. The positive polarity time (positively polarized wire-electrode) has the purpose of promoting the metal transfer via the current pulse, and, in the case of aluminum, this is the time that the oxide layer is removed by cathodic cleaning [4]. The negative current provides an increase in the wire melting rate because of the effect of arc climbing [5].

For this version of the process, the number of parameters that must be defined, as well as the waveform variations, make configuration difficult and time-consuming. For this reason, the development of a methodology for calculating

the configuration parameters, which provide a synergistic relationship between the process variables, is of utmost importance. Based on the aforementioned reasoning and the lack of deeper scientific knowledge about the selection of proper variables for the process and its operation, this paper proposes a calculation method that allows synergistic parameterization for AC-pulsed GMAW of aluminum.

### 1.1 Theoretical fundamentals of the calculation of the parameters for AC-pulsed GMAW

The main motivation for the development of a synergistic program for welding processes is the need to simplify the power source adjustment, thus diminishing the number of parameters input by the operator. A large number of the synergistic versions commercially available possess a single parameter as input data (usually wire feed speed or average current) and, depending on the manufacturer, there are also parameters related to corrections, for arc length for example. For AC-pulsed GMAW, apart from a current or wire feed speed input, it is interesting that one of the input parameters is the negative electrode percentage (%EN). This offers the operator a wider variety of configurations for different levels of heat input.

A fundamental aspect to be considered in AC-pulsed GMAW is the difference between the wire melting rate in each of the polarities, which can result in wire melting imbalance and, consequently, in arc length instability. In their research, which evaluated AC-pulsed GMAW parameterization, Park et al. [6] analyzed this problem first. In general, to maintain arc length stability, the first step is the determination of the wire melting rate in the positive and negative polarities (EP and EN), relative to the current. With the knowledge of melting rate variation and the corresponding compensation, it is possible to maintain the wire

feed speed constant, despite the fact that the negative polarity has a higher melting rate. The difference is compensated by distinct adjustments of the current level applied in each phase (EN and EP).

To achieve optimized stability in the process, several aspects must be considered, such as the pulse parameters most suitable to obtain ODPP detachment, the moment of the drop detachment, and the most appropriate type of waveforms, among other things. In most cases, the pulse parameters utilized are the same as the DC-pulsed GMAW. However, regarding waveform type, several possibilities are found in the literature [7], each one possessing particularities that, sometimes, contradict the others.

In research that evaluated the metal transfer mode in DC-pulsed GMAW for 4043 aluminum alloy welding wire, Dutra et al. [8] found that the drop detachment, at the initial moments of the base current, provided good results. At this moment, the drop is not subjected to the electromagnetic forces related to the high current level (pulse), which leads to a smoother detachment and impingement into the pool. Based on this philosophy, the use of a waveform without a positive base time would not fit this application. Moreover, in the researches of Vilarinho et al. [9] for steel, and Bohme et al. [7] for aluminum, it was observed that a waveform without a positive base current cannot obtain satisfactory stability, and in the case of aluminum, it was observed that there is almost no cathodic cleaning. The research of Scotti and Monteiro [10] and Ueyama et al. [11] make reference to the use of a waveform that has a positive base before and after the pulse. Vilarinho et al. [9] even quote the use of a waveform with a positive base only before the pulse, which has an effect on the drop detachment during the pulse.

The definition of a synergistic program for automatic configuration of the welding parameters of the power source starts with the selection of the welding wire, the wire diameter, and the shielding gas utilized. With this combination it is possible to establish the remaining variables that condition the process for arc stability and adequate metal transfer. Generally, the extracted parameters of this combination are: wire melting rate relative to welding current (in both positive and negative polarity), the pulse parameters ( $I_p$  and  $t_p$ ) which are chosen according to the ODPP condition, and drop diameter. These parameters are considered to be fixed in the calculation throughout the whole application range of the process for the given configuration. The research of Vilarinho et al. [9] and Scotti and Monteiro [10] for steel, also define the positive base current as a fixed parameter, which follows a stability criterion ( $I_b > 20$  A). Scotti and Monteiro [10] also utilize the envisaged average positive current ( $I_{A+}$ ) as an input parameter and only  $I_p$  as a fixed parameter. Both studies show good results for AC-pulsed GMAW of steel. However, some information about the calculation evokes doubts. Vilarinho

et al. [9] utilize the simpler waveform (consisting only of positive pulse and negative base) as a pattern for calculation, not clarifying the definition of some parameters when other waveforms with positive base current are used. Scotti and Monteiro [10] state in their methodology that the drop diameter values should be close to the electrode diameter (1.2 mm in that case), but their results indicate drop diameters that vary from 1.4 to 1.7 mm.

## 2 Applied methodology

The methodology for defining the parameters of the AC-pulsed GMAW process was developed with the objective of ensuring arc stability, consistent metal transfer, and also a good weld bead aspect. It is known that the wire melting rate increases with negative polarity, which leads to arc length change. Therefore, a prediction was made for the wire melting rate for both polarities (EP and EN) by the wire consumption Eq. (1). Knowledge of these melting rate variations is needed to equate the wire feed speed on positive and negative polarities. Since aluminum shows low resistivity (displayed in Eq. 1 by  $\beta$ ), this equation can be expressed by the first portion, which results in linear Eq. (2):

$$W_{fs} = \alpha \times I_A + \beta \times I_{RMS}^2 \times L \quad (1)$$

$$W_{fs} = \alpha \times I_A \quad (2)$$

The  $\alpha$  coefficient was defined separately for each polarity, and the procedure to obtain it consisted of bead on plates trials using only positive polarity to determine  $\alpha_+$  and only negative polarity for  $\alpha_-$ . The deposits to evaluate the process were conducted on a 3.0 mm thick 1100 aluminum workpiece, and the welding wire utilized was 5087 aluminum alloy 1.2 mm in diameter. The shielding gas was pure argon, with a flow rate of 13.0 l min<sup>-1</sup>, and the contact tip to work distance (CTWD) was 15.0 mm. The welding was done in the flat position with a 5° pushing angle for the torch and a welding speed ( $W_s$ ) of 0.4 m min<sup>-1</sup>. The voltage, current, and wire feed speed signals, were measured using a portable acquisition system known as SAP 4.0, with a 5 kHz acquisition rate. These same welding configurations were then utilized to evaluate the AC-pulsed GMAW process, and high-speed filming was performed. The average values of the  $\alpha$  coefficient, calculated from linear regression of the average values for current ( $I_A$ ) and wire feed speed ( $W_{fs}$ ), which were obtained from monitoring experiments, were:  $\alpha_+ = 0.051$  m min<sup>-1</sup> A<sup>-1</sup> and  $\alpha_- = 0.129$  m min<sup>-1</sup> A<sup>-1</sup>.

In order to determine the waveform parameters, a rectangular waveform was taken as a starting point, whereby two waveform types were defined: type (I) has pulse—positive base current—negative base current; and type (II) has

**Table 1** Calculated parameters for AC-pulsed GMAW

%EN	$I_p$ (A)	$t_p$ (ms)	$I_b$ (A)	$t_b$ (ms)	$I_n$ (A)	$t_n$ (ms)	$W_{fs}$ (m min <sup>-1</sup> )
30 %	350	1.2	24	10	23	4.8	3
	350	1.2	33	7.2	31	3.6	4
	350	1.2	43	5.5	39	2.9	5
	350	1.2	54	4.4	47	2.4	6
30 %	430	0.8	30	10.4	23	4.8	3
	430	0.8	41	7.6	31	3.6	4
	430	0.8	53	5.9	39	2.9	5
	430	0.8	66	4.8	47	2.4	6
50 %	350	1.2	7	6.8	23	8	3
	350	1.2	11	4.8	31	6	4
	350	1.2	14	3.6	39	4.8	5
	350	1.2	18	2.8	46	4	6
50 %	430	0.8	18	7.2	23	8	3
	430	0.8	24	5.2	31	6	4
	430	0.8	32	4	39	4.8	5
	430	0.8	40	3.2	47	4	6

positive base current—pulse—positive base current—negative base current; since these allow for the ODPP detachment to occur in the positive base current, after the pulse.

Some parameters are invariable during the process and were utilized as input parameters to calculate the other ones. Among them are: negative wire melting rate coefficient ( $\alpha_-$ ), positive wire melting rate coefficient ( $\alpha_+$ ), pulse current ( $I_p$ ), pulse time ( $t_p$ ), drop diameter ( $d_d$ ), wire diameter ( $d_w$ ), and negative electrode percentage (%EN). The pulse parameters ( $I_p$  and  $t_p$ ) were the same as those utilized for the DC-pulsed GMAW, which ensured ODPP detachment soon after the pulse, at the positive base current. The parameters defined were:  $I_p = 430$  A with  $t_p = 0.8$  ms; and  $I_p = 350$  A with  $t_p = 1.2$  ms. Each one of the two groups of variables was evaluated for two negative electrode percentage levels (EN = 30, 50 %) for a drop diameter of 1.2 mm. The remaining variables to be defined were calculated for equations utilizing the input parameters.

The negative current is calculated by the relation between the expected  $W_{fs}$  and the negative polarity wire melting rate, using Eq. (3); and the negative time is calculated from Eq. (4), according to the desired %EN. The drop detachment period T is calculated from the desired drop diameter, the utilized wire diameter, and the wire feed speed, as shown in Eq. (5).

$$W_{fs} = I_n \times \alpha_{(-)} \tag{3}$$

$$t_n = \frac{T \times NE\%}{100} \tag{4}$$

$$T = \frac{40 \times d_d^3}{d_w^2 \times W_{fs}} \tag{5}$$

The base current is defined by the formula in Eq. (6), and the  $I_{A+}$  value required for this calculus is defined by Eq. (7). The base current time is calculated based on the period and negative time already found, by means of Eq. (8).

$$I_b = \frac{[I_{A+} \times (t_p + t_b) - (I_p \times t_p)]}{t_b} \tag{6}$$

$$W_{fs} = I_{A+} \times \alpha_{(+)} \tag{7}$$

$$t_b = T - t_p - t_n \tag{8}$$

### 3 Results and discussions

Applying the proposed methodology, the parameters listed in Table 1 were found for type I and II waveforms for a wire feed speed range from 3 to 6 m min<sup>-1</sup>. To perform the tests with waveform type II, the base time was simply divided by 2, whereas each half was placed before and after the pulse. The tests with parameters  $I_p = 350$  A,  $t_p = 1.2$  ms, and EN = 50 %, were not evaluated due to the calculated base current being too low, which would invalidate the process.

#### 3.1 First set of pulse parameters: $I_p = 350$ A and $t_p = 1.2$ ms

In the first analysis, using the pulse parameters  $I_p = 350$  A,  $t_p = 1.2$  ms, and EN = 30 %, weld beads of satisfactory quality were obtained in addition to an oscillogram featuring repeatability and the presence of a voltage peak which indicates drop detachment at the positive base current,

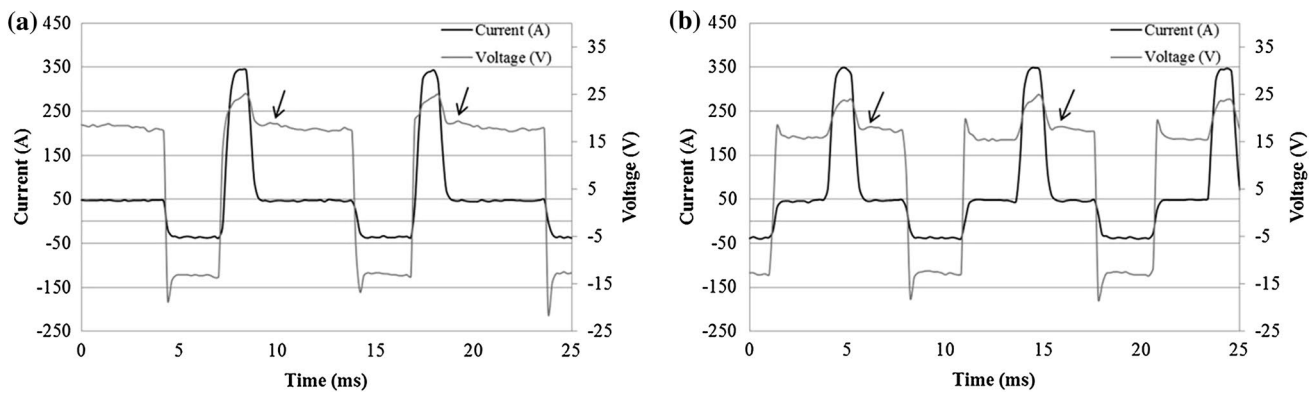


**Fig. 2** Current and voltage oscillograms using  $W_{fs} = 5 \text{ m min}^{-1}$  and  $EN = 30 \%$  for **a** waveform I and **b** waveform II

**Fig. 3** Weld bead relative to Fig. 1's oscillograms for **a** waveform I and **b** waveform II

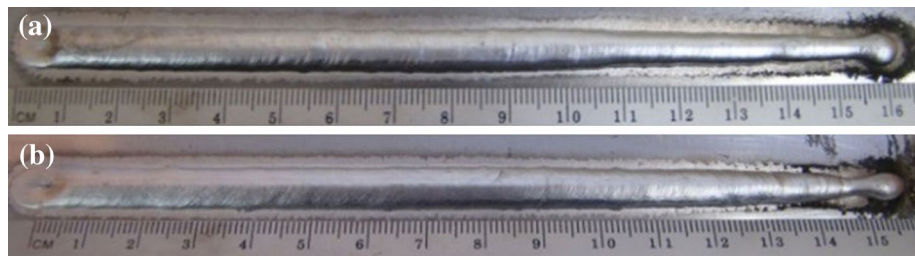


**Table 2** Wire feed speed, root mean square of the current, and power for  $I_p = 350 \text{ A}$ ,  $t_p = 1.2 \text{ ms}$ , and  $EN = 30 \%$

$W_{fs}$ (m $\text{min}^{-1}$ )	$I_{RMS}$ (A)	$P$ (W)
<b>Waveform I</b>		
3	90	1077
3.9	105	1332
4.9	119	1578
5.9	131	1853
<b>Waveform II</b>		
3.1	95	1030
4	110	1253
4.9	124	1551
5.9	138	1880

thus adequately, as shown on Fig. 2. In Fig. 3, the weld bead images relative to Fig. 2's oscillograms can be seen. It should be remarked that the weld beads being narrower at their beginning is a consequence of plate heating/bead-plate wetting along the execution of the weld. Since the aluminum plate is at room temperature before welding and the heat conduction is high, the first portions of the weld bead do not properly wet the plate. As the plate becomes warmer along the welding, the wettability of the bead improves.

Table 2 presents the results for the wire feed speed ( $W_{fs}$ ), power ( $P$ , automatically calculated through Eq. 9, using instant and synchronized current and voltage values), and root mean square current ( $I_{RMS}$ ), measured in each experiment.

$$P = \frac{\sum_{i=1}^n U_i I_i}{n} \tag{9}$$

Given the results, it can be stated that there is no expressive difference in current and power values between the waveforms, meaning that both waveforms I and II could, in principle, be applied to this process for a certain welding application.

According to the high-speed video images of Fig. 4a, it is possible to observe the sequence of drop detachment, consistent with the ODPP premise of stability. For waveform I, at some moments during the metal transfer there were occurrences of secondary drops with small diameters close to the detachment, which can be seen in detail in Fig. 4b.

### 3.2 Second set of pulse parameters: $I_p = 430 \text{ A}$ and $t_p = 0.8 \text{ ms}$

From the results related to the pulse parameters  $I_p = 430 \text{ A}$  and  $t_p = 0.8 \text{ ms}$ , a larger negative polarity time can be seen. Figure 5 shows the oscillogram of both waveform types analyzed for  $EN = 30 \%$ , while Fig. 6 shows this for  $EN = 50 \%$ . For both conditions it was possible to observe the voltage peak related to the drop detachment, after the pulse. In Fig. 7, the ODPP detachment can be seen by means of high-speed videography, as can the arc climbing phenomenon which is typical of the negative polarity.

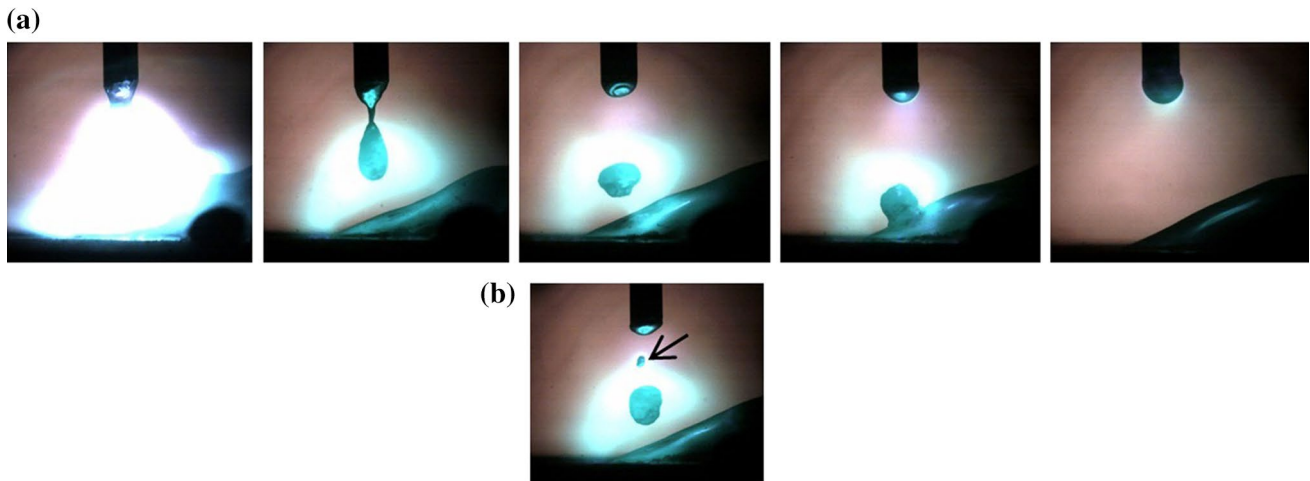


**Fig. 4** Detachment sequence images from high-speed camera: **a** ODPP detachment of oscillogram from Fig. 2; and **b** detailed formation of secondary drop

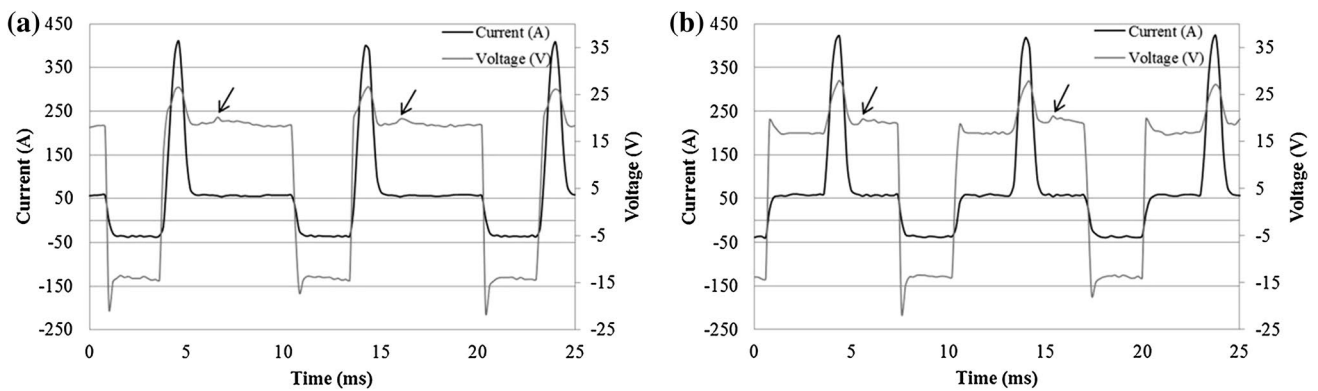


**Fig. 5** Current and voltage oscillograms using  $I_p = 430$  A,  $t_p = 0.8$  ms, EN = 30 %, and  $W_{fs} = 5$  m min<sup>-1</sup> for **a** waveform I and **b** waveform II

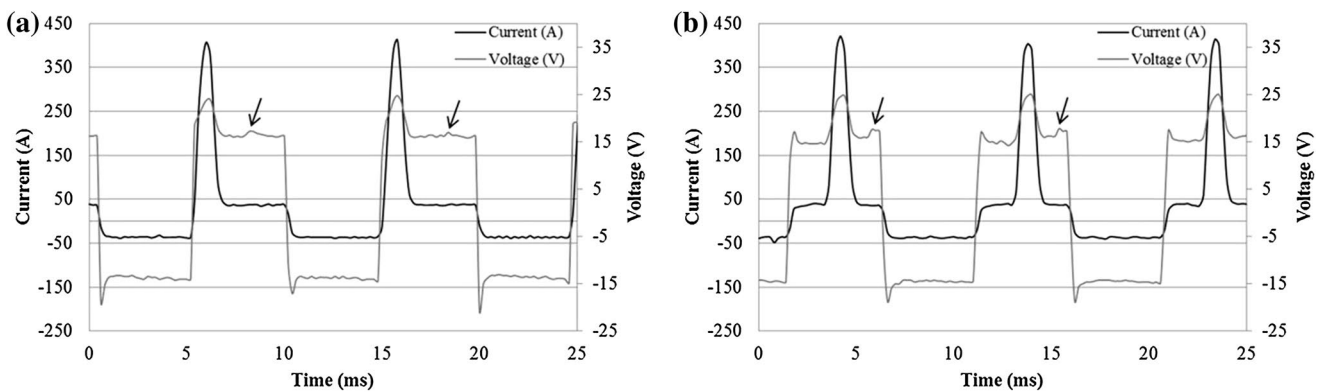


**Fig. 6** Current and voltage oscillograms using  $I_p = 430$  A,  $t_p = 0.8$  ms, EN = 50 %, and  $W_{fs} = 5$  m min<sup>-1</sup> for **a** waveform I and **b** waveform II

As for the weld bead aspect, there was no significant difference in the results utilizing either waveform types for the same %EN, as seen in Figs. 8 and 9. What can

be observed is a greater wetting of the weld beads when using EN = 30 % as opposed to 50 %, since the process remains in positive polarity for longer, thus increasing the

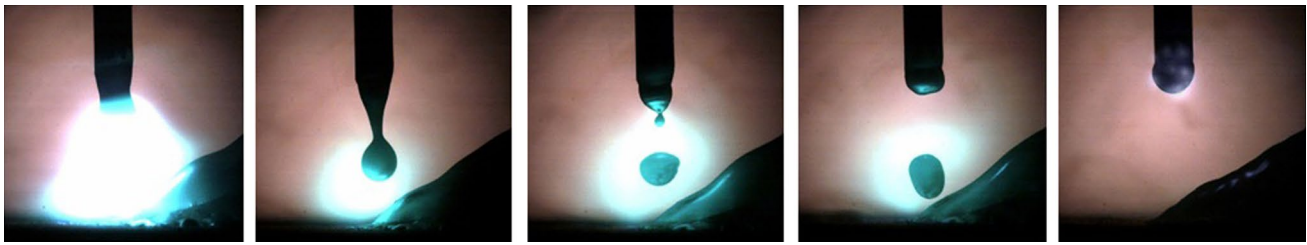


**Fig. 7** High-speed camera images for  $I_p = 430$  A,  $t_p = 0.8$ , EN = 50 %, and  $W_{fs} = 5$  m min<sup>-1</sup>

**Fig. 8** Weld bead related to Fig. 5's oscillograms for **a** waveform I and **b** waveform II

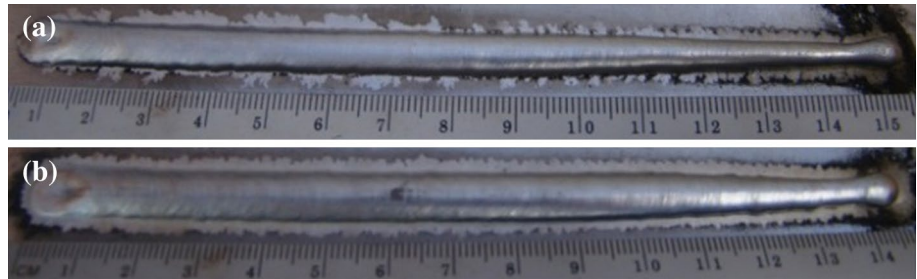
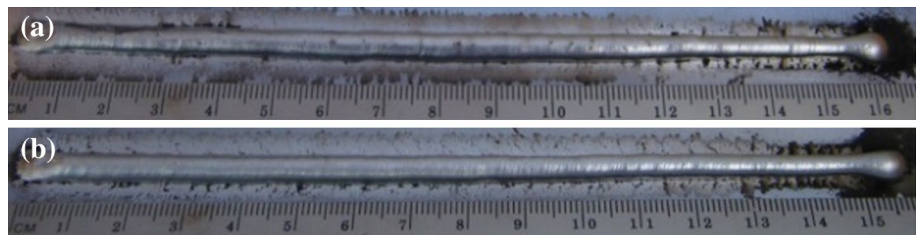


**Fig. 9** Weld bead related to Fig. 6's oscillograms for **a** waveform I and **b** waveform II



input of heat into the workpiece. Table 3 shows the  $W_{fs}$ ,  $P$ , and  $I_{RMS}$  values of each experiment, and it can be seen that EN = 30 % results in higher power for the process.

In the experiments with EN = 50 %, it was possible to observe moments of instability in the process, with the occurrence of short-circuiting due to arc length variation, which may have been caused by the larger negative polarity time.

As can be seen in Table 4, with the wire feed speed kept at approximately 5 m min<sup>-1</sup>, it was possible to decrease the electrical power by 330 W (a reduction of about 20 %) when increasing the negative electrode percentage from 30 to 50 %. Compared to DC-pulsed GMAW with a wire feed speed of 4.8 m min<sup>-1</sup>, the decrease in power is around 500 W (30 % reduction).

### 3.3 Process performance at higher wire feed speeds

In order to widen the observation range of the process, experiments with higher wire feed speed were also done with the parameters set to  $I_p = 430$  A and  $t_p = 0.8$  ms, and EN = 30 and 50 %, with the objective being the possible application in filler and cover passes in groove joints. Figure 10

depicts oscillograms for the pulse parameters configured to  $I_p = 430$  A and  $t_p = 0.8$  ms, for an 8 and 10 m min<sup>-1</sup> wire feed speed and EN = 30 %, while Fig. 11 depicts the same welding condition for EN = 50 %. In the case of EN = 30 %, the arc remained stable as in the experiments with lower wire feed speed, and the drop detachment moment was evident on the oscillograms. For EN = 50 %, however, it was noticed that, as the wire feed speed is increased, the drop detachment is no longer regular and repeatable, whereby there are no evident peaks of drop detachment. The shorter positive polarity time was not enough for the drop to detach. Arc instability was observed for EN = 50 %, whereas the alternative was adjusting the arc length by reducing the wire feed speed. These results are shown in Table 5, which depicts the measured values of  $W_{fs}$ ,  $I_{RMS}$ , and  $P$ .

## 4 Conclusions

The suggested methodology allows a synergistic calculation for AC-pulsed GMAW, by obtaining the required parameters for welding with this version of the process. In

**Table 3** Wire feed speed, root mean square of the current, and power for  $I_p = 430$  A and  $t_p = 0.8$  ms

$W_{fs}$ (m min <sup>-1</sup> )	$I_{RMS}$ (A)	$P$ (W)
EN = 30 %		
Waveform I		
3	81	1053
4	100	1263
4.9	113	1563
5.9	125	1842
Waveform II		
3.1	90	1017
4	107	1276
4.9	121	1664
5.9	137	1871
EN = 50 %		
Waveform I		
3	83	833
4	99	1030
4.8	111	1233
5.6	121	1446
Waveform II		
3.1	89	809
4.1	104	1055
4.9	116	1360
5.8	130	1569

**Table 4** Comparative power values for DC- and AC-pulsed GMAW processes (EN = 30 and 50 %)

Process	$W_{fs}$ (m min <sup>-1</sup> )	$I_{RMS}$ (A)	$P$ (W)
DC P GMAW	4.8	112	1728
AC P GMAW 30 %	4.9	113	1563
AC P GMAW 50 %	4.8	111	1233

the tested wire feed speed ranges, the ODPP detachment condition was obtained for both waveforms (I and II), with stability and similar results for power and RMS current. In accordance with the philosophy of the drop detachment at the start of the base current, waveform I has advantages over waveform II, because the positive base time after the pulse of the latter is shorter compared to the former, and, as the wire feed speed is increased, the drop detachment moment approaches the polarity inversion.

For both pulse parameter sets analyzed ( $I_p = 430$  and 350 A) no difference could be observed regarding process stability. What could be analyzed and quoted as an advantage of using the higher pulse current (430 A) is the fact that it is possible to reach the lowest levels of average current.

In the experiment with EN = 50 % for higher wire feed speeds, the process was unstable, with short-circuiting occurring at speeds higher than 6 m min<sup>-1</sup> because of the arc length variation. The weld beads presented less wetting when compared to the experiments with EN = 30 %. This is accounted for by the heat input reduction that happens at longer negative polarity times. For the RMS of currents up to 130 A that were analyzed in this research, EN = 50 % offers better results in applications such as the welding of thin plates. For applications that require higher material deposition with low heat input, the best options were found to be with EN = 30 %, since a stable process at wire feed speeds up to 10 m min<sup>-1</sup> could be achieved.

It was assumed, as a simplification, that the EN effects are present during the entire EN time and only during this time, not considering inertial or delayed effects. Although it is known that there are some effects on the arc that are not completely in phase with variations of the arc parameters, the high-speed videos show that for the context of the present work, no appreciable discrepancy or influence of this kind could be noticed.

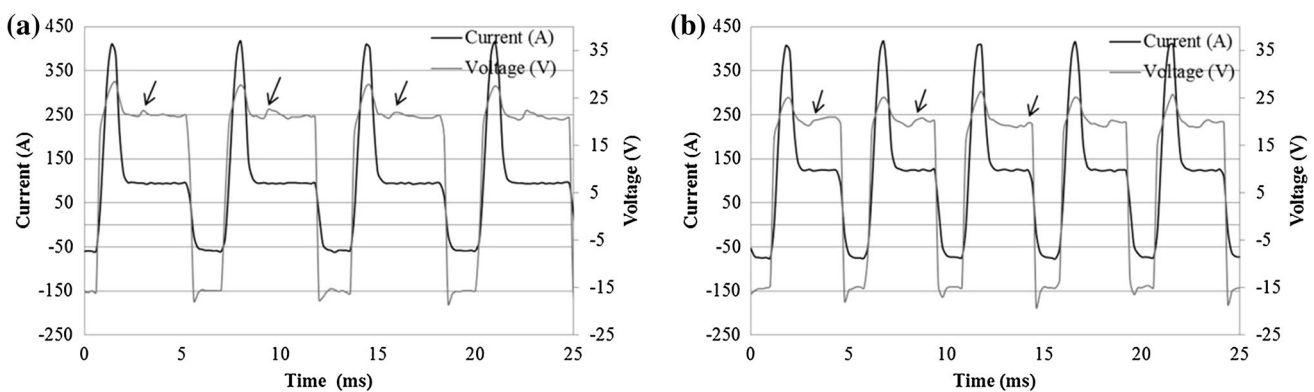


**Fig. 10** Current and voltage oscillograms using  $I_p = 430$  A,  $t_p = 0.8$  ms, and EN = 30 % for: **a**  $W_{fs} = 8$  m min<sup>-1</sup> and **b**  $W_{fs} = 10$  m min<sup>-1</sup>



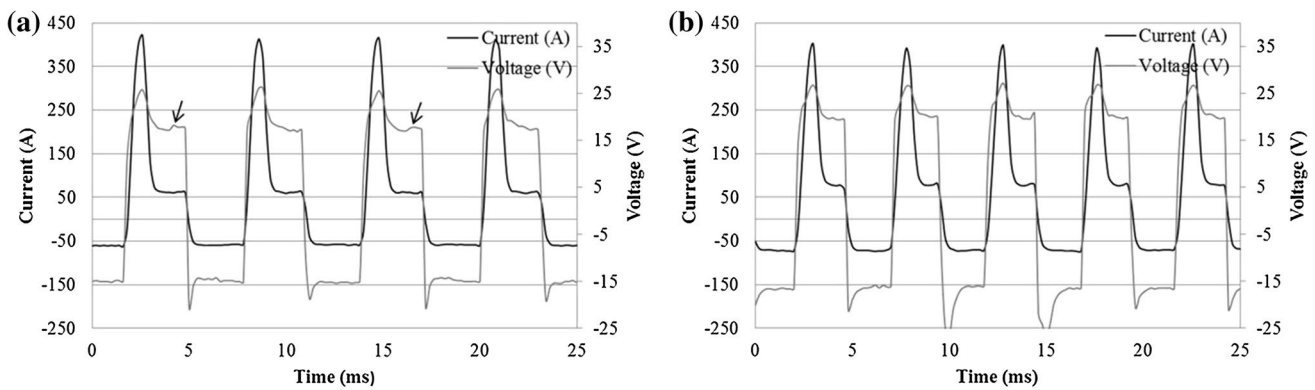


**Fig. 11** Current and voltage oscillograms using  $I_p = 430$  A,  $t_p = 0.8$  ms, and EN = 50 % for: **a**  $W_{fs} = 8$  m min<sup>-1</sup> and **b**  $W_{fs} = 10$  m min<sup>-1</sup>

**Table 5** Wire feed speed, power, and the root mean square of the current for  $I_p = 430$  A and  $t_p = 0.8$  ms

Set $W_{fs}$ (m min <sup>-1</sup> )	Read $W_{fs}$ (m min <sup>-1</sup> ) <sup>a</sup>	$I_{RMS}$ (A)	$P$ (W)
EN = 30 %			
Waveform I			
7	7	140	2250
8	7.8	148	2544
9	8.9	162	2830
10	9.8	174	2978
EN = 50 %			
Waveform II			
7	6.6	135	1812
8	7.4	145	1973
9	8.1	150	2244
10	8.6	159	2557

<sup>a</sup> Set value was adjusted (reduced) during welding to avoid short-circuiting in order to maintain stability

The AC-pulsed GMAW version developed in this work resulted in a synergic welding program, already implemented in a in-house developed power source and was successfully applied in the aluminum sailboat construction.

## References

- Kumar R, Dilthey U, Dwivedi DK, Ghosh PK (2009) Thin sheet welding of Al 6082 alloy by AC pulse-GMA and AC wave pulse-GMA welding. *Mater Des* 30:306–313. doi:10.1016/j.matdes.2008.04.073
- Tong H, Ueyama T, Harada S, Ushio M (2001) Quality and productivity improvement in aluminium alloy thin sheet welding using alternating current pulsed metal inert gas welding system. *Sci Technol Weld Join* 6(4):203–208. doi:10.1179/136217101101538776
- Palani PK, Murugan N (2006) Selection of parameters of pulsed current gas metal arc welding. *J Mater Process Technol* 172:1–10J. doi:10.1016/j.jmatprotec.2005.07.013
- Scotti A, Dutra JC, Ferraresi VA (2000) The influence of parameter settings on cathodic self-etching during aluminum welding. *J Mater Process Technol* 100(1–3):179–187
- Lancaster JF (1979) Metal transfer in Fusion Welding. In: *Welding Institute Conference on Arc Physics and Weld Pool Behavior*, USA, pp 135–146
- Park HJ, Kim DC, Kang MJ (2013) The arc phenomenon by the characteristic of EN ratio in AC pulse GMAW. *Int J Adv Manuf Technol* 66(5–8):867–875. doi:10.1007/s00170-012-4371-1
- Böhme D, Rosenfeld W, Baum L, Cramer H (2002) MIG-Welding of Very Thin Al-Sheets by A.C. Pulsed Arc. *IIW-Document-No. XII-1720-02*, 8p
- Dutra JC, Marques C, Silva RHG (2012) Interpretative agreements and disagreements in the interrelationships of the variables of the pulsed current applied to the aluminum wire 4043. *Soldag Insp* 17(3):201–209. doi:10.1590/S0104-92242012000300004
- Vilarinho LO, Nascimento AS, Fernandes DB, Mota AM (2009) Methodology for parameter calculation of VP-GMAW. *Weld J* 88(4):92–98 ISSN: 00432296
- Scotti A, Monteiro LS (2012) A methodology for parameterization of the AC MIG/MAG process. *Soldag Insp* 17(3):271–277 ISSN: 0104-9224
- Ueyama T, Tong H, Harada S, Passmore R, Ushio M (2005) AC pulsed GMAW improves sheet metal joining. *Weld J* 84(2):40–46 ISSN: 00432296